

Water Cages as Chemical Reactors: VUV Photolysis of Dimethyl Ether Clathrate Hydrate Thin Films in Ultrahigh Vacuum

Bijesh K. Malla^{1,4}, Soham Chowdhury¹, Khushboo Bhardwaj³, Rajnish Kumar^{4,5} and Thalappil Pradeep^{1,2*}*

¹DST Unit of Nanoscience (DST UNS) and Thematic Unit of Excellence (TUE), Department of Chemistry, Indian Institute of Technology Madras, Chennai 600036, India,

²International Centre for Clean Water, IIT Madras Research Park, Chennai 600113, India

³Department of Chemistry, Indian Institute of Technology Madras, Chennai 600036, India

⁴Department of Chemical Engineering, Indian Institute of Technology Madras, Chennai 600036, India

⁵School of Sustainability, Indian Institute of Technology Madras, Chennai 600036, India

Corresponding authors

***Email:** pradeep@iitm.ac.in, rajnish@iitm.ac.in

Instrumentation

Experimental Setup

In this study, all experiments were conducted in an ultrahigh vacuum (UHV) instrument (with a base pressure of $\sim 5 \times 10^{-10}$ mbar) discussed in detail in our previous literature.^{1,2} The instrument consists of three UHV chambers (namely ionization, octupole, and scattering) and is equipped with reflection absorption infrared spectroscopy (RAIRS), low-energy ion scattering (LEIS), temperature-programmed desorption (TPD) mass spectrometry, Cs⁺ ion-based secondary ion mass spectrometry (SIMS), along with a vacuum ultraviolet (VUV) lamp (Figure 1). Six turbomolecular pumps maintain the vacuum chambers' base pressure, which is supplemented by several oil-free diaphragm pumps. The chamber pressure is monitored by a Bayard-Alpert gauge, controlled by a MaxiGauge vacuum gauge controller (Pfeiffer, Model TPG 256 A).

A highly polished Ru(0001) single crystal was used as the substrate to create thin ice films, which was mounted on a copper holder. It was connected to a helium cryostat (Cold Edge technology), which could maintain a temperature as low as 8 K. A resistive heater (25 Ω), controlled by a temperature controller (Lakeshore 336), was used to heat the substrate to 1000 K. The substrate temperature was measured using a K-type thermocouple sensor with an accuracy of ± 0.5 K. Repeated heating to 400 K before each vapor deposition ensured a clean surface suitable for the current study. It is worth noting that the surface has a negligible role in the current study as our experiments were on multilayer ice films.

RAIRS and TPD-MS Setup

In this study, the thermal processing of vapor-deposited ice samples was monitored using RAIRS (Reflection-Absorption Infrared Spectroscopy) and TPD-MS (Temperature Programmed Desorption-Mass Spectrometry). The RAIRS data were collected in the 4000-550 cm^{-1} range with a spectral resolution of 2 cm^{-1} , using a Bruker FT-IR spectrometer called Vertex 70. The ice sample was exposed to an incident angle of $80^\circ \pm 7^\circ$ by focusing the IR beam through a ZnSe viewport. The reflected IR beam from the sample was detected using a liquid-nitrogen-cooled mercury-cadmium-telluride (MCT) detector. To prevent absorption by atmospheric moisture, the IR beam outside the vacuum chamber was purged with dry N₂. Each RAIR spectrum was obtained by

averaging over 512 scans to improve the signal-to-noise ratio. An Extrel quadrupole mass spectrometer was used for TPD-MS in an out-of-sight configuration.

VUV Source

A deuterium lamp (McPherson, Model 634, with MgF₂ window, 30 W) of vacuum ultraviolet (VUV) range 115-400 nm was used as the UV light source (Figure S11). The VUV lamp was differentially pumped and attached to the UHV chamber through the MgF₂ window (with a cut-off at ~114 nm (10.87 eV)). This design enables the source to emit light at incredibly short wavelengths, reaching as far as 115 nanometers. The UV lamp flux was determined by applying the widely used ozone method (O₂ → O₃ conversion), where solid O₂ was photolyzed by VUV radiation at 10 K. The average photon flux reaching the ice sample was estimated to be $\sim 6 \times 10^{12}$ photons cm⁻²s⁻¹.^{3,4}

SIMS Setup

Cs⁺-based secondary ion mass spectrometry (SIMS) was used to identify and monitor surface reactions on DME ice. Cs⁺ ions (m/z = 133) were selected for their high depth resolution (~1 bilayer) and sensitivity to neutral surface species.⁵⁻⁷ Reactive ion scattering (RIS) experiments were performed using 60 eV Cs⁺ ions generated by a low-energy alkali gun. Upon impact, Cs⁺ ions form adducts with neutral surface molecules via ion-dipole interactions and eject them along the outgoing trajectory. The resulting Cs⁺-molecule adducts were analyzed using a quadrupole mass spectrometer. Neutral photoproducts were identified by subtracting the Cs⁺ mass (m/z = 133) from the detected adduct masses.

Materials and Sample Preparation

DME (Sigma Aldrich, 99.9% purity) was purchased from Sigma Aldrich and used without further purification. Water (H₂O) (18.2 MΩ resistivity) and deuterated water (D₂O) (Sigma Aldrich, 99.9% purity) was taken in a vacuum-sealed test tube (with a glass-to-metal seal) and was further purified by several freeze-pump-thaw cycles. To prepare 150 ML of DME, the chamber was filled with DME vapor for 5 min at a pressure of 5×10^{-7} mbar. 300 ML of DME-water/deuterated water was prepared by backfilling the chamber with vapors of DME and water/deuterated water for 10 min at a pressure of 5×10^{-7} mbar.

Supporting Information 1

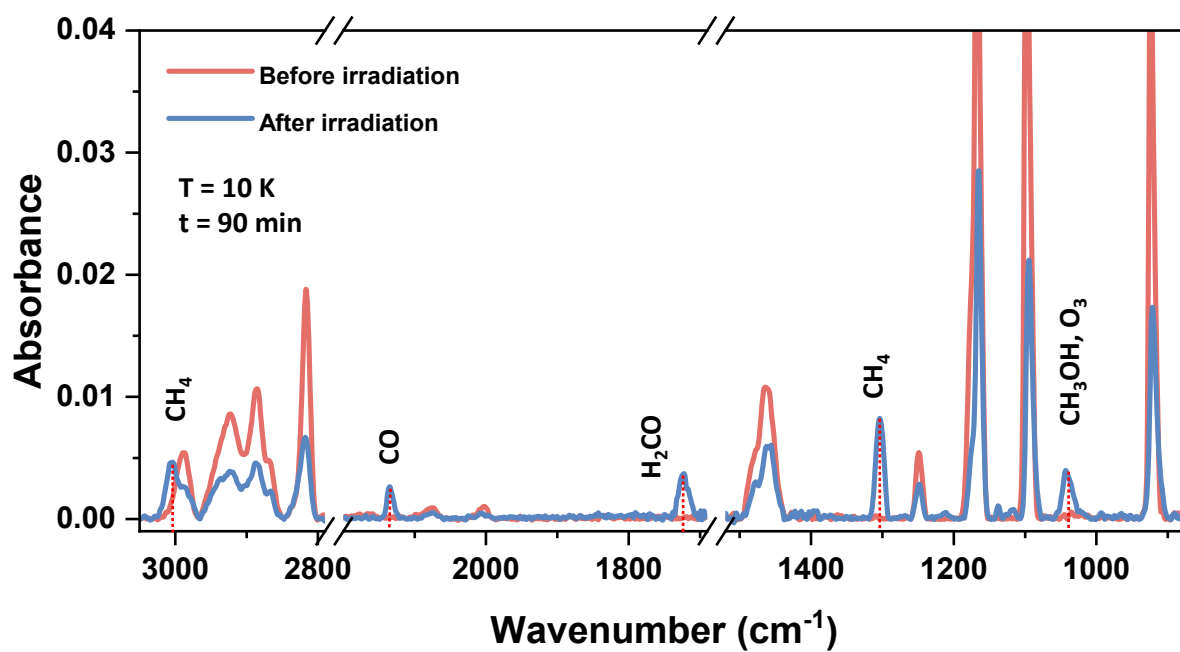


Figure S1. RAIR spectra of 150 ML of pure DME ice before and after VUV irradiation.

Supporting Information 2

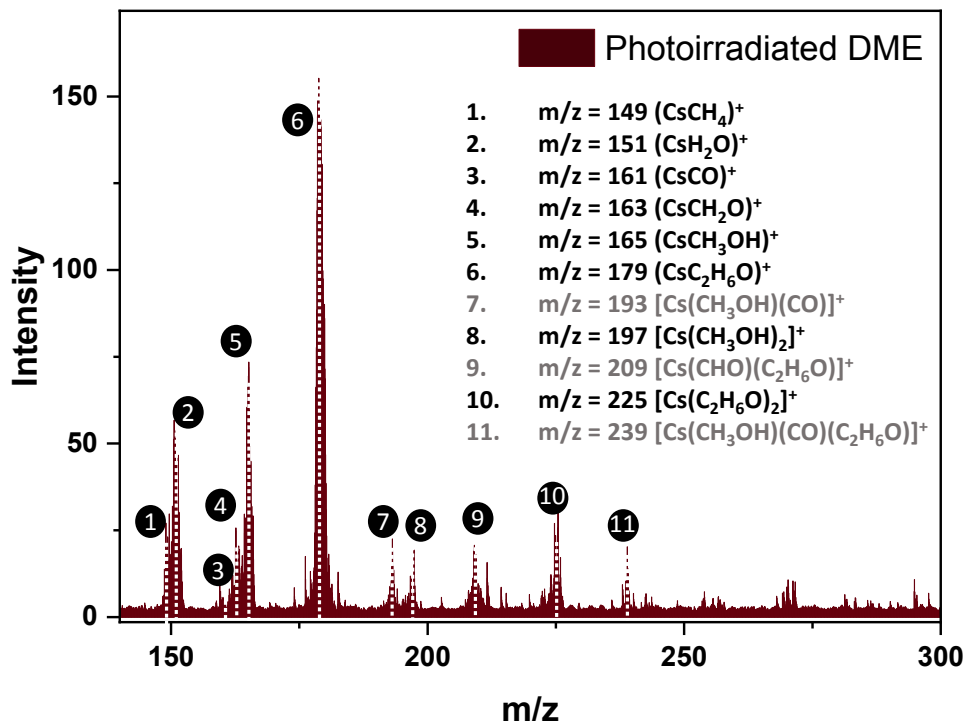


Figure S2. Reactive ion scattering (RIS) mass spectrum obtained after 90 min of VUV irradiation of amorphous DME ice. The mass spectrum of the irradiated ice was obtained by colliding the sample with 60 eV Cs^+ ions at 10 K. All the RIS photoproducts have been assigned, as listed in the panel. The mass peaks highlighted in grey are assigned with lower confidence.

Supporting Information 3

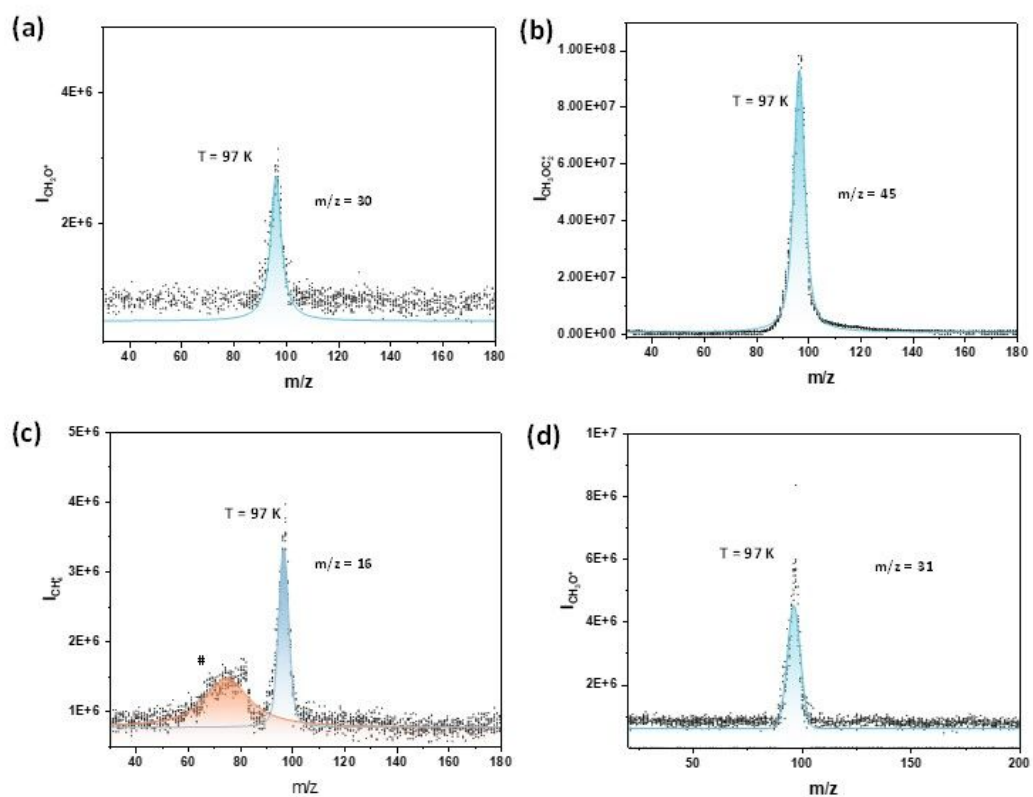


Figure S3. TPD-MS spectra of photoirradiated 150 ML of DME ice. Sublimation profiles using integrated ion counts at (a) $m/z = 30$, in (b) $m/z = 45$, in (c) $m/z = 16$ and (d) $m/z = 31$ are plotted.

Supporting Information 4

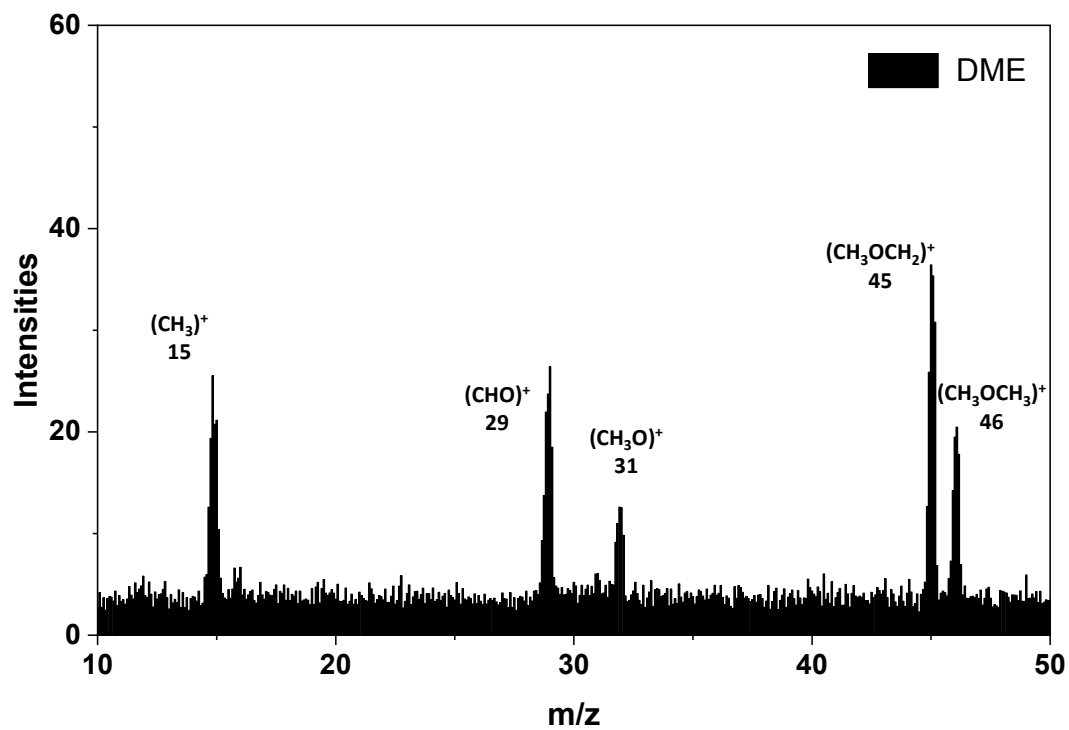


Figure R1. Gas-phase electron ionization mass spectrum of DME.

Supporting Information 5

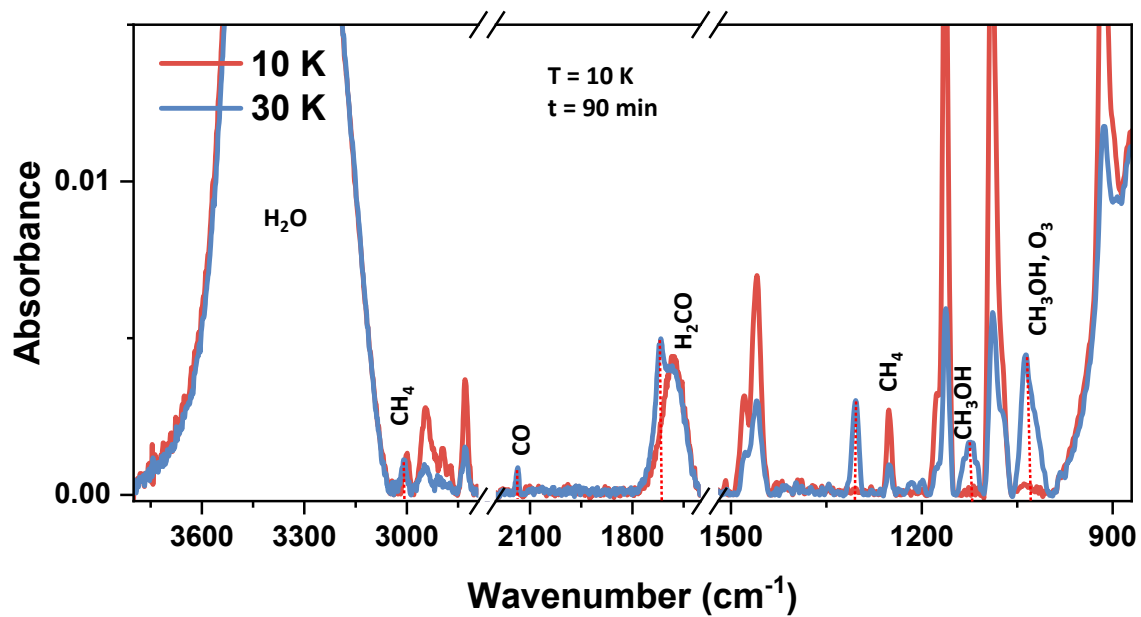


Figure S5. RAIR spectra of 300 ML of DME-water ice mixture before and after VUV irradiation.

Supporting Information 6

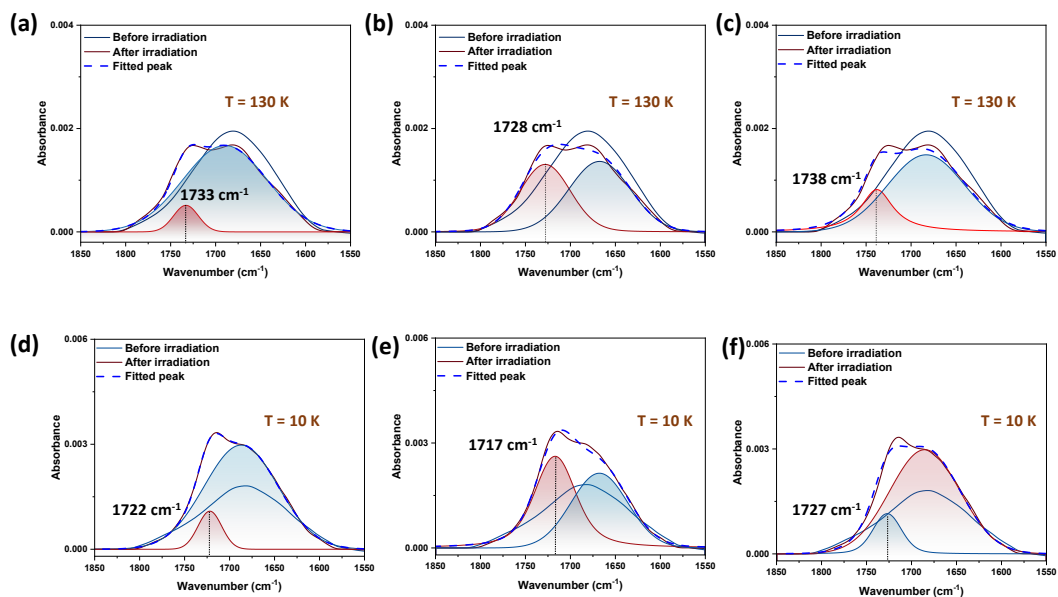


Figure S6. RAIR spectra of DME CH before and after 90 min of irradiation in the O–H bending region. Panels (a–c) show spectra recorded at 130 K, while panels (d–f) correspond to 10 K. In panels (a–d), the post-irradiation spectra are deconvoluted into two components: the red shaded contribution, assigned to formaldehyde (C=O stretching region), and the blue shaded contribution, assigned to water. At 130 K (a–c), three different peak centers (1733, 1728, and 1738 cm^{-1}) are considered for the formaldehyde fitting. At 10 K (d–f), three different peak centers (1722, 1717, and 1727 cm^{-1}) are considered for the formaldehyde fitting.

Supporting Information 7

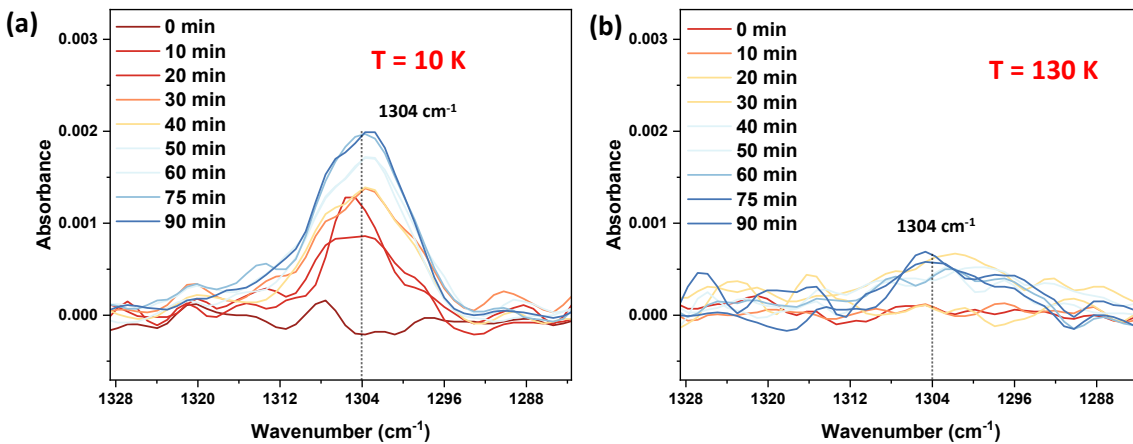


Figure S7. RAIR spectra of CH₄ in the C-H asymmetric bending mode, photoproduced by VUV irradiation of DME CH at (a) 10 K and (b) 130 K. DME CH was prepared by annealing a DME–water mixture at 130 K for 2 h. For panel (a), the system was subsequently cooled to 10 K prior to irradiation, whereas for panel (b), irradiation was performed directly at 130 K.

Supporting Information 8

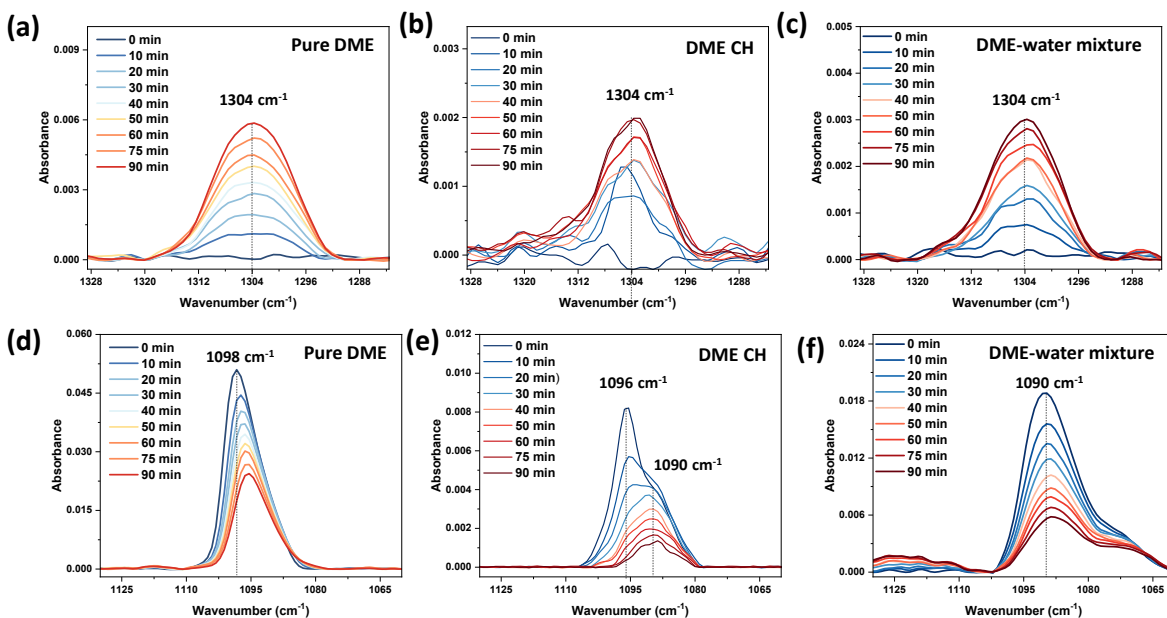


Figure S8. Time-dependent RAIR spectra of VUV-irradiated pure DME, DME CH, and DME–water mixtures at 10 K. Panels (a–c) show the RAIR spectra of photoproducted CH₄ from (a) pure DME, (b) DME CH, and (c) DME–water mixtures, monitored via the C–H asymmetric bending mode. Panels (d–f) present the RAIR spectra of DME for (d) pure DME, (e) DME CH, and (f) DME–water mixtures in the C–O antisymmetric stretching region.

Supporting Information 9

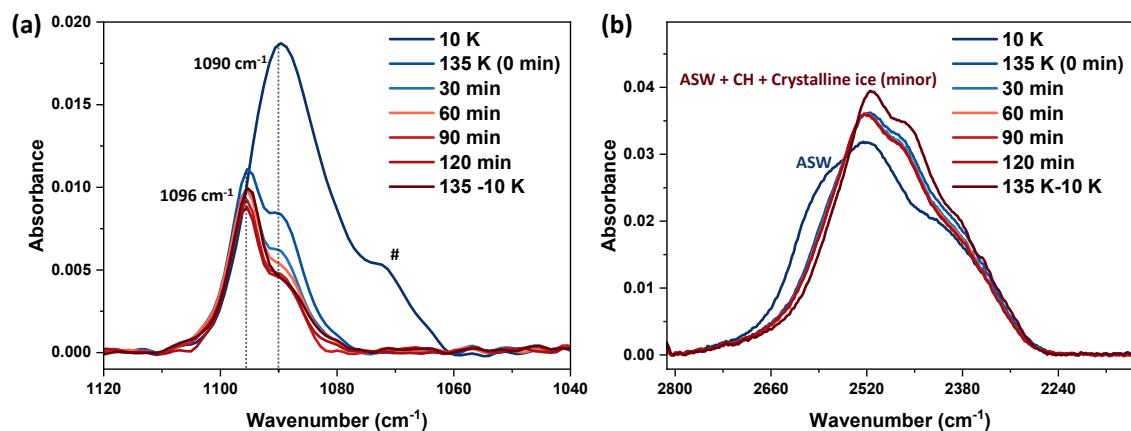


Figure S9. The formation of DME CH was investigated using RAIR spectroscopy. DME-D₂O CH was prepared by vapor co-deposition onto a Ru(0001) substrate at 10 K, followed by annealing at 135 K for 2 h. (a) RAIR spectra of the DME-D₂O ice mixture in the C-O antisymmetric stretching region are shown. The broad feature marked by the symbol (#) corresponds to hydrogen-bonded DME molecules. (d) RAIR spectra of the DME-D₂O ice mixture in the O-D stretching region are shown.

Supporting Information 10

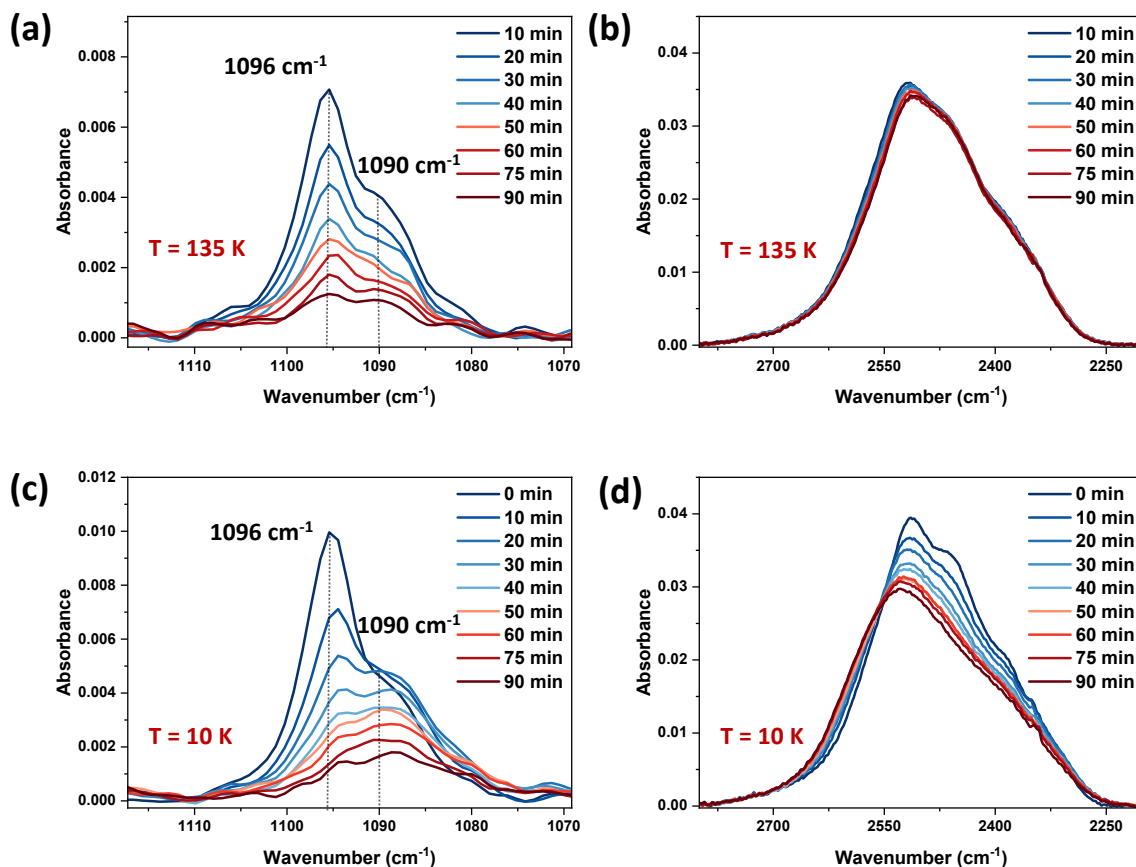


Figure S10. Time-dependent RAIR spectra of VUV-irradiated deuterated DME CH at 135 K (a, b) and 10 K (c, d). Panels (a) and (c) show the RAIR spectra in the C–O antisymmetric stretching region at 135 K and 10 K, respectively. Panels (b) and (d) present the RAIR spectra in the O–D symmetric stretching region at 135 K and 10 K, respectively.

Supporting Information 11

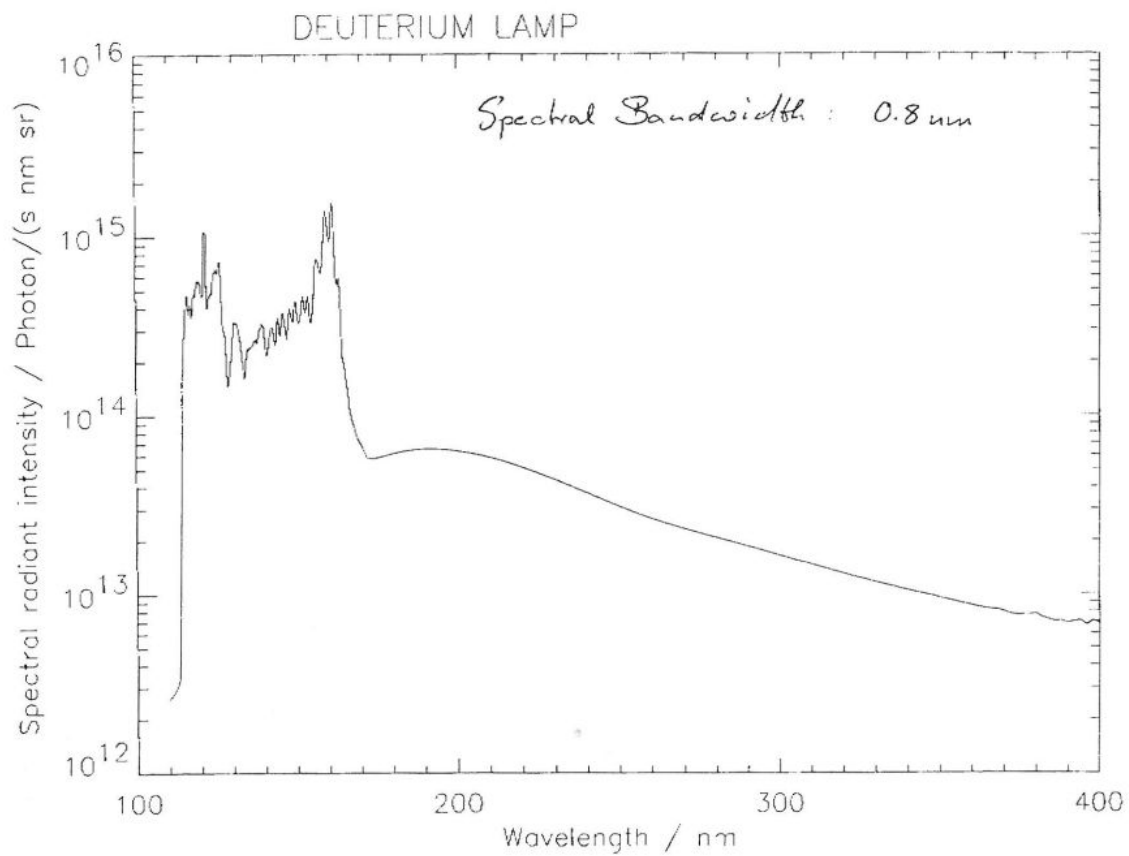


Figure S11. Emission spectrum of Model 634 Deuterium lamp, provided by the McPherson.

References

- (1) Bag, S.; Bhuin, R. G.; Methikkalam, R. R. J.; Pradeep, T.; Kephart, L.; Walker, J.; Kuchta, K.; Martin, D.; Wei, J. Development of Ultralow Energy (1–10 eV) Ion Scattering Spectrometry Coupled with Reflection Absorption Infrared Spectroscopy and Temperature Programmed Desorption for the Investigation of Molecular Solids. *Rev. Sci. Instrum.* **2014**, *85* (1), 1–7. <https://doi.org/10.1063/1.4848895>.
- (2) Vishwakarma, G.; Ghosh, J.; Pradeep, T. Desorption-Induced Evolution of Cubic and Hexagonal Ices in an Ultrahigh Vacuum and Cryogenic Temperatures. *Phys. Chem. Chem. Phys.* **2021**, *23* (41), 24052–24060. <https://doi.org/10.1039/D1CP03872A>.
- (3) Vishwakarma, G.; Malla, B. K.; Chowdhury, S.; Ghosh, J.; Methikkalam, R. R. J.; Kumar, R.; Pradeep, T. Ultraviolet Photolysis of CO₂ Clathrate Hydrate and H₂O–CO₂ Mixed Ice under Ultrahigh Vacuum. *Phys. Chem. Chem. Phys.* **2025**, *27* (21), 11025–11035. <https://doi.org/10.1039/D5CP00620A>.
- (4) Malla, B. K.; Chowdhury, S.; Paliwal, D.; K. M., H.; Vishwakarma, G.; Methikkalam, R. R. J.; Pradeep, T. Simulated Interstellar Photolysis of N₂O Ice: Selectivity in Photoproducts. *J. Phys. Chem. C* **2025**, *129* (2), 1120–1128. <https://doi.org/10.1021/acs.jpcc.4c06624>.
- (5) Cyriac, J.; Pradeep, T.; Kang, H.; Souda, R.; Cooks, R. G. Low-Energy Ionic Collisions at Molecular Solids. *Chemical Reviews*. American Chemical Society October 10, 2012, pp 5356–5411. <https://doi.org/10.1021/cr200384k>.
- (6) Kang, H.; Kim, K. D.; Kim, K. Y. Molecular Identification of Surface Adsorbates. Reactive Scattering of Hyperthermal Cs⁺ from a Ni(100) Surface Adsorbed with CO, C₆H₆, and H₂O. *J. Am. Chem. Soc.* **1997**, *119* (49), 12002–12003. <https://doi.org/10.1021/JA970246C/ASSET/IMAGES/LARGE/JA970246CF00002.JPEG>.
- (7) Kang, H.; Shin, T. H.; Park, S. C.; Kim, I. K.; Han, S. J. Acidity of Hydrogen Chloride on Ice. *J. Am. Chem. Soc.* **2000**, *122* (40), 9842–9843. <https://doi.org/10.1021/ja000218l>.